

Stefano Ramat · R. John Leigh · David S. Zee ·
Lance M. Optican

Ocular oscillations generated by coupling of brainstem excitatory and inhibitory saccadic burst neurons

Received: 29 July 2003 / Accepted: 16 May 2004 / Published online: 28 July 2004
© Springer-Verlag 2004

Abstract The human saccadic system is potentially unstable and may oscillate if the burst neurons, which generate saccades, are not inhibited by omnipause neurons. A previous study showed that combined saccade vergence movements can evoke oscillations in normal subjects. We set out to determine: 1) whether similar oscillations can be recorded during other paradigms associated with inhibition of omnipause neurons; 2) whether lesions of the fastigial nuclei disrupt such oscillations; and 3) whether such oscillations can be reproduced using a model based on the coupling of excitatory and inhibitory burst neurons. We recorded saccadic oscillations during vergence movements, combined saccade-vergence movements, vertical saccades, pure vergence and blinks in three normal subjects, and in a patient with saccadic hypermetria due to a surgical lesion affecting both fastigial nuclei. During combined saccade-vergence, normal subjects and the cerebellar patient developed small-amplitude ($0.1\text{--}0.5^\circ$), high-frequency (27–35 Hz), conjugate horizontal saccadic oscillations. Oscillations of a similar amplitude and frequency occurred during blinks, pure vergence and vertical saccades. One normal subject could generate saccadic oscillations voluntarily ($\sim 0.7^\circ$ amplitude, 25 Hz) during sustained convergence. Previous models proposed that high-frequency eye oscillations produced by the saccadic system (saccadic oscillations), occur because of a delay in a

negative feedback loop around high-gain, excitatory burst neurons in the brainstem. The feedback included the cerebellar fastigial nuclei. We propose another model that accounts for saccadic oscillations based on 1) coupling of excitatory and inhibitory burst neurons in the brainstem and 2) the hypothesis that burst neurons show post-inhibitory rebound discharge. When omnipause neurons are inhibited (as during saccades, saccade-vergence movements and blinks), this new model simulates oscillations with amplitudes and frequencies comparable to those in normal human subjects. The finding of saccadic oscillations in the cerebellar patient is compatible with the new model but not with the recent models including the fastigial nuclei in the classic negative-feedback loop model. Our model proposes a novel mechanism for generating oscillations in the oculomotor system and perhaps in other motor systems too.

Keywords Brainstem · Burst neurons · Postinhibitory rebound discharge · Saccadic mechanism · Saccadic oscillations

Introduction

Voluntary shifts of gaze are achieved by rapid, conjugate eye movements called saccades. Saccades require a pulse-step change in muscle innervation to overcome the viscous drag and elastic restoring force of orbital tissues (Robinson and Keller 1972). The pulse is primarily due to neurons in the reticular formation of the brain stem that discharge intensely (burst) with saccades (Van Gisbergen et al. 1981; Scudder et al. 2002; Sparks 2002). For horizontal saccades, excitatory burst neurons in the paramedian pontine reticular formation (PPRF) project monosynaptically to ipsilateral abducens internuclear and motoneurons that excite yoked agonist muscles, whereas inhibitory burst neurons in the rostral medulla project to contralateral abducens internuclear and motoneurons that disfacilitate yoked antagonist muscles (Strassman et al. 1986a, b; Horn et al. 1995). Burst neuron activity is gated by omnipause

S. Ramat (✉) · D. S. Zee
Department of Neurology, The Johns Hopkins University,
Pathology Building, Suite 2-210, 600 N. Wolfe Str.,
Baltimore, MD 21231, USA
e-mail: stefano@dizzy.med.jhu.edu
Tel.: +1-410-9552904

R. J. Leigh
Department of Neurology, Veterans Affairs Medical Center and
University Hospitals, Case Western Reserve University,
Cleveland, OH, USA

L. M. Optican
Laboratory of Sensorimotor Research, National Eye Institute,
NIH,
Bethesda, MD, USA

neurons (OPN) lying in the pontine nucleus raphe interpositus (RIP) (Büttner-Ennever et al. 1988); OPN are tonically active during fixation and suppress activity during all saccades (Keller 1974; Evinger et al. 1982). OPN are also inhibited during saccadic-vergence movements, and blinks (Collewijn et al. 1985; Hain et al. 1986; Hepp et al. 1989; Zee and Hain 1992; Mays and Gamlin 1995; Mays and Morrissette 1995; Scudder et al. 2002; Busetini and Mays 2003).

In humans, the mechanism that generates saccades is potentially unstable, and may lead to high-frequency, conjugate oscillations, occurring one after the other without any intervening period of steady fixation. These are saccadic oscillations (Zee and Robinson 1979; Van Gisbergen et al. 1981) and are thought to be driven by the same burst neurons that generate saccades because the dynamic properties of the individual eye movements that comprise the oscillations correspond to those of voluntary saccades (Shults et al. 1977; Hotson 1984; Ashe et al. 1991; Yee et al. 1994). In healthy human subjects, the saccadic system is usually inhibited by OPN; they prevent the saccadic mechanism from oscillating when steady fixation is desired. However, even in some normal subjects, brief, high-frequency, saccadic oscillations occur especially when accompanied by a blink (Hain et al. 1986; Rottach et al. 1998). Some normal subjects can induce saccadic oscillations voluntarily ('voluntary nystagmus') (Shults et al. 1977; Hotson 1984). Most normal subjects develop small-amplitude saccadic oscillations when a small saccade and large vergence movement are combined (Ramat et al. 1999). In certain diseases, pathological involuntary saccadic oscillations—flutter or opsoclonus—are prominent (Ashe et al. 1991; Leigh and Zee 1999; Bhidayasiri et al. 2001).

The first question we sought to answer was whether similar oscillations can be observed during several paradigms causing the inhibition of the OPN; thus, we recorded combined saccade-vergence eye movements, pure vergence, blinks and vertical saccades in a group of normal subjects. We found that saccadic oscillations of similar amplitudes and frequencies were recorded in all such conditions.

Previous models of the saccadic mechanism require a delay in the negative feedback loop controlling saccade amplitude to produce saccadic oscillations (Zee and Robinson 1979; Van Gisbergen et al. 1981). Such a feedback loop was later hypothesized to pass through the cerebellar fastigial nuclei (Lefevre et al. 1998; Wong et al. 2001) and around the brainstem saccade generator. Thus, the second aim here was to determine whether a cerebellar patient with a bilateral fastigial nuclei lesion had oscillations, since the models with a feedback loop through the fastigial nucleus predict he should not. The cerebellar patient also showed saccadic oscillations having similar characteristics to those recorded in the normal subjects. These findings lead to two possible explanations: either saccadic oscillations are generated through a different mechanism, independent of the integrity of the

local feedback loop, or the fastigial nuclei are not part of such a loop.

Thus, the third aim here was to propose a new model for saccadic oscillations and to simulate saccadic oscillations that occur in different paradigms associated with OPN inhibition. The new model accounts for oscillations in normal subjects, and in a patient with a fastigial nucleus lesion because a delay in the negative feedback loop passing through the cerebellar fastigial nuclei is not needed for the new model to oscillate. Our model is based on the positive feedback loops that are intrinsic in the brainstem connectivity of excitatory and inhibitory burst neurons (Strassman et al. 1986a, b; Scudder 1988) and on postinhibitory rebound discharge (Huguenard 1998; Aizenman and Linden 1999; Perez-Reyes 2003)

Methods

The data were obtained at both the Cleveland Veterans Affairs Medical Center (Lab 1) and at the Johns Hopkins Hospital (Lab 2). The recordings were performed in two separate laboratories purely for convenience; nonetheless, this arrangement allowed us to confirm that the eye oscillations were unlikely due to instrumentation, recording techniques or data analysis artifacts. There are small differences in the arrangement of the experimental conditions of the two labs, which are reported for scientific accuracy, but do not detract from the purposes of the experiments.

Eye movement recordings

Eye movements were recorded with the magnetic field/search coil technique in both laboratories.

In Lab 1 horizontal and vertical movements of both eyes were measured using 6-ft field coils (CNC engineering, Seattle, WA, USA). Coil signals were hardware low-pass filtered (bandwidth 0–150 Hz), to avoid aliasing, prior to digitization at 500 Hz with 16-bit resolution. These digitized coil signals were filtered with an 80-point Remez FIR filter (bandwidth 0–100 Hz). Details of the data recording and signal processing techniques used in Lab 1 were previously described (Ramat et al. 1999).

In Lab 2 the movements of both eyes were recorded around all three axes of rotation (horizontal, vertical, and torsional) using the magnetic field/search coil method with dual coil annuli. The output signals of the coils were hardware filtered with a single pole RC filter with bandwidth of 0–90 Hz, and then sampled at 1,000 Hz with 12-bit resolution. Further details of the calibration and recording procedures can be found in (Bergamin et al. 2001).

Subjects and patient

We studied three normal subjects in a set of experimental conditions that had been reported previously to elicit transient saccadic oscillations. Our normal subjects ranged from 31–56 years in age. One subject (C1) was recorded in Lab 1, two (B1-B2) in Lab 2. One subject recorded in Lab 2 (B2) was able to generate, at will, conjugate oscillations during sustained vergence.

We also studied (Lab 1) a 50-year-old man (P1) in whom a cerebellar astrocytoma had been resected 6 years previously. Clinical examination demonstrated marked bilateral hypermetria of horizontal saccades, as well as bilateral limb ataxia (worse on his left side). Smooth-pursuit eye movements were impaired. He had childhood esotropia with left amblyopia, but retained some ability to converge his eyes. He showed hypermetria of horizontal saccades made to visual targets (the initial saccade had median gain 1.26 over all trials). For saccades (tested up to 20°), the relationships between amplitude and peak velocity, and between amplitude and duration were similar for the cerebellar patient and normal subjects. These are typical characteristics of saccades with lesions of the fastigial nuclei (Robinson and Fuchs 2001).

We defined the extent of his cerebellar lesion from magnetic resonance imaging scans (Fig. 1), using the atlas of Duvernoy (1995). The lesion bilaterally involved the culmen of the vermis, the fastigial nuclei including the caudal parts, and the emboliform nuclei, with partial involvement of the dentate nuclei. The uvula, nodulus, quadrangular lobules, and left superior cerebellar peduncles were also involved.

All our subjects and the patient gave informed consent prior to participating in our experimental recordings. The study was conducted in accordance with the tenets of the 1964 Declaration of Helsinki and was approved by the Institutional Review Boards of the Cleveland Veterans Affairs Medical Center and of the Johns Hopkins Hospital.

Experimental paradigm

Lab 1

The visual stimuli were a red laser spot (the “far target”) rear-projected onto a semi-translucent tangent screen at a viewing distance of 1.2 m and a green LED (the “near target”) located at a distance, calculated for each subject, to require 10° of vergence (typically at about 35 cm). The LED was positioned so that, in the horizontal plane, it was aligned with the far target for either the right or the left eye (Müller paradigm), or on the subject’s midline.

We used three experimental paradigms:

- 1) Müller paradigm. Subjects shifted their line of sight between the near and far targets, aligned horizontally on one eye, but requiring a vertical saccade of about 10°; the near target was near vertical zero position and the far target was approximately 10° higher. Each

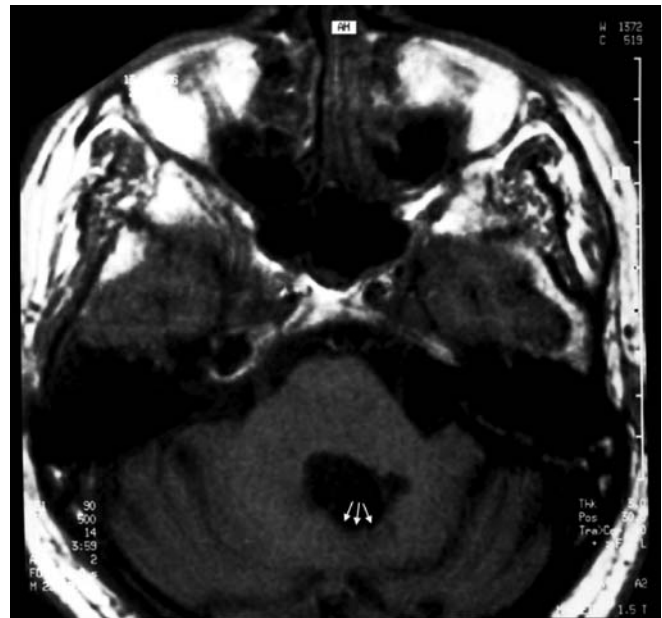


Fig. 1 Axial magnetic resonance image (TR: 500; TE: 14) of the cerebellar patient in the plane of the middle cerebellar peduncles and the anterior superior cerebellar fissure, showing a large surgical midline lesion (indicated by arrows) in the structures above the roof of the fourth ventricle. Based on 3-mm sections, the lesion was demonstrated to extend above and below the median dorsal recess, and involve the fastigial nuclei, including the caudal parts (see text for details)

eye was tested in turn. Each gaze shift was prompted by illumination of either the near or far target, with a 100-ms gap; each target light remained illuminated for 2.4 s to allow time for subjects to fix upon it. This paradigm stimulated asymmetrical horizontal saccadic-vergence movements in combination with a vertical saccade. In a prior study (Ramat et al. 1999), it was shown that the Müller paradigm was a reliable experimental strategy to induce saccadic oscillations in normal subjects.

- 2) Midline vergence. The subjects shifted gaze between far and near targets lying on their midsagittal plane and separated vertically by about 10°.
- 3) Vertical saccades. Subjects made large vertical saccades (20–40°) between targets aligned on their midsagittal plane.

Lab 2

Saccadic oscillations were investigated in an additional two normal subjects (B1, B2), one being able to produce voluntary, conjugate oscillations.

The stimuli were two red LEDs at a viewing distance of 190 cm (the “far target”) and 15 cm (the “near target”) which, depending on the interpupillary distance (IPD) of each patient, required about 22° of vergence (for a typical IPD of 6 cm).

Four paradigms were used with these subjects:

- 1) Müller paradigm. The subject was positioned so that, in the horizontal plane, the near and far LEDs were

aligned with either the right or the left eye, with a minimal vertical displacement between the two targets to allow the subject to view both LEDs.

- 2) Midline vergence. Subjects were asked to perform gaze shifts between the near and far targets aligned on their midsagittal plane.
- 3) Blinks. Subjects were asked to perform pure blinks during steady fixation of the far target.
- 4) Vertical saccades. Subjects were asked to perform large vertical saccades (20–40°) between targets aligned on their midsagittal plane.

A fifth paradigm was performed by subject B2 who was asked to produce voluntary conjugate oscillations associated with sustained convergence effort.

Data analysis

Although saccadic oscillations were seen in the position traces, their amplitudes were small (<1° in most cases); accordingly, we chose to study the oscillations using eye velocity, for which the frequency is unaltered and the amplitudes are enhanced by a factor proportional to their frequency. The velocity traces were analyzed interactively to detect periods of sustained oscillations; these data segments were marked for further analysis. Saccadic oscillations often were superimposed on an ongoing slower eye movement, equivalent to a drift superimposed on the oscillations. To deal with this problem, the selected eye-velocity data were fit initially with a straight line to identify the baseline drift, which was then subtracted from the raw data ('detrend'). The periodic oscillations were harmonically distorted; thus, their amplitude and frequency were measured by finding the best-fitting (in the least-squared error sense) sine wave ($a\sin(2\pi ft + \theta)$), using the Matlab implementation of the Nelder-Mead simplex method. Each fitted function was visually checked for agreement with the data. Thus, the values of amplitude and frequency for each analyzed oscillation were taken as the a and f parameters of the fitting function, respectively. To provide a measure of the quality of the estimated parameters, we computed 95% confidence intervals for the parameters of the fit and considered the amplitude of such intervals. Note that the error of the estimate provided by the fit is statistically likely to be less than half of the

reported amplitude of the confidence interval. All oscillations that could be fit with a single sinusoidal function for at least 1.5 periods were considered.

The model (see Appendix) was simulated with Matlab/Simulink on an IBM-compatible personal computer. The periodic oscillation produced by the model was analyzed with the same fitting technique that was used to characterize the experimental data. Statistical significance of comparisons of both intra- and inter-subject data was assessed using the rank-based Wilcoxon test and the Student's t -test. When the two results disagreed (<5% of measurements) the distribution of the data was examined using the resampling based bootstrap technique (Efron and Tibshirani 1993). The t -test result was chosen when the distribution was Gaussian, the Wilcoxon value otherwise. Statistical significance was considered to be attained at $P < 0.05$ unless otherwise specified. Using representative data collected from normal subjects (C1 and B1) during the Müller paradigm, we computed the minimum sample size (n) required from each of the two populations to estimate the difference between the two means (either intra- or inter-subject) with a 95% confidence interval being not wider than the confidence interval found for the parameters of the fit (see above). We found $n = 13$. Thus, we chose 13 as the threshold sample size for considering the data valid for statistical comparison.

Results

The frequency and the velocity amplitude of saccadic oscillations for each subject, in each tested experimental condition, are summarized in Table 1. Eye velocity was calculated from the cyclopean eye ((right eye + left eye)/2). Values are the mean \pm SD (standard deviation) of the identified periods of sustained oscillations. The amplitude and frequency of saccadic oscillations varied over time even within a single trial as can be noted both in Fig. 2 (patient P1) and in Fig. 3 (patient P1 and subject C1).

The quality of the estimated amplitude and frequency parameters was best (i.e., the amplitude of the 95% confidence interval was smallest) for the subject who could generate voluntary oscillations (at most 2 Hz and 5°/s). The ranges of the confidence intervals for the parameters of the fits of the patient data were, at most,

Table 1 Characteristics of the oscillations over all experiments. Mean \pm SD frequency and amplitude (measured on velocity traces) of oscillations recorded in each subject and each experimental condition

Subject	Müller	Vertical saccades	Blinks	Midline vergence
P1	35 \pm 4 Hz; 23 \pm 6°/s	36 \pm 4 Hz; 21 \pm 7°/s	N.T.	35 \pm 4 Hz; 20 \pm 4°/s
C1	32 \pm 4 Hz; 16 \pm 6°/s	33 \pm 5 Hz; 14 \pm 3°/s	33 \pm 5 Hz; 13 \pm 3°/s	32 \pm 5 Hz; 13 \pm 3°/s
B1	35 \pm 4 Hz; 15 \pm 3°/s	32 \pm 5 Hz; 17 \pm 4°/s	34 \pm 5 Hz; 16 \pm 3°/s	N.S.
B2	27 \pm 4 Hz; 41 \pm 16°/s	25 \pm 4 Hz; 47 \pm 16°/s	27 \pm 4 Hz; 18 \pm 5°/s	26 \pm 3 Hz; 23 \pm 7°/s

N.T. indicates that the subject was not tested in that specific experimental condition. *N.S.* indicates that the number of identified saccadic oscillations for the subject in the specific experimental condition was less than 13. *Müller* Müller paradigm, *Vertical saccades* vertical saccades along midsagittal plane, *Blinks* blinks alone, *Midline vergence* vergence movements between targets aligned on the midsagittal plane

Fig. 2a-c Example of high-frequency saccadic oscillations made by the cerebellar patient during a combined saccade-vergence movement. Far and near targets were aligned on one eye (Müller paradigm). **a** Both horizontal and vertical individual eye velocities. **b** The horizontal (continuous black) and vertical (dash-dotted) version velocity traces. The grey trace offset from the others shows the detrended sinusoidal oscillation. **c** The version (continuous line) and vergence (dashed line) position traces

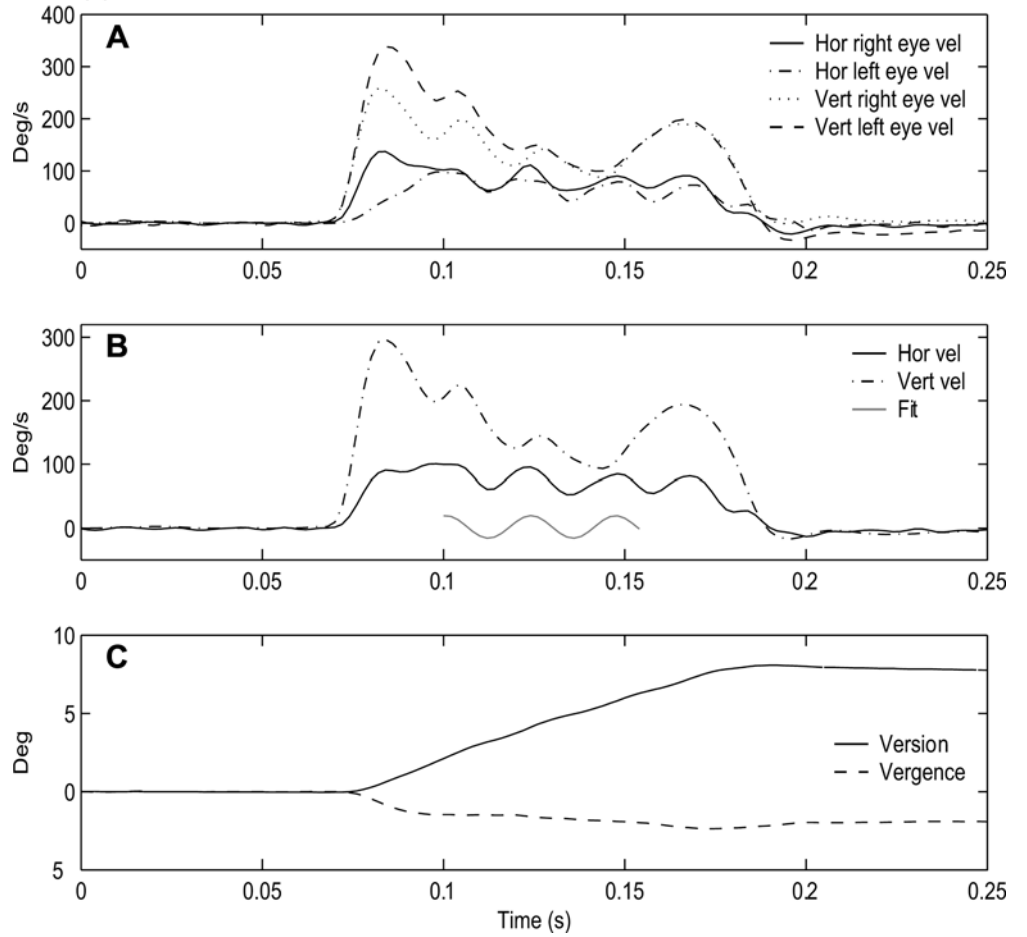
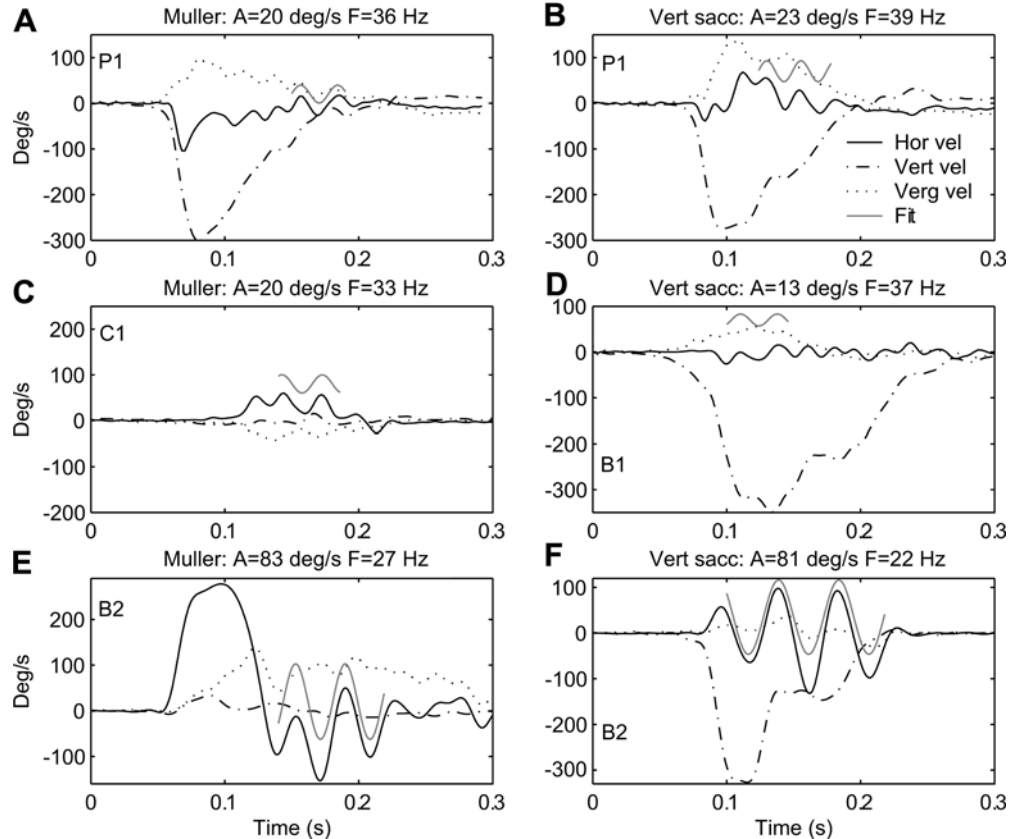


Fig. 3a-f Responses to Müller and midline paradigms. Examples showing horizontal saccadic oscillations in normal subjects and the patient. Each panel shows the vertical (dash-dotted) and horizontal (continuous black) version velocity traces and the detrended sinusoidal oscillation (grey). **a, b** Data from the cerebellar patient. **c, d** Data from two normal subjects (C1 and B1). **e, f** Data from the subject who could produce ‘voluntary nystagmus’. **a, c, e** Müller paradigm (far and near targets aligned on one eye). **b, d, f** Vertical saccade paradigm. The title of each panel indicates the condition, the amplitude (A) and frequency (F) of the identified sinusoid



6 Hz and 6°/s, whereas those of the control subjects were, at most, 6 Hz and 7°/s and 4 Hz and 4°/s (C1 and B1, respectively).

The responses to each experimental paradigm are summarized below by describing their general characteristics and specifying the differences among subjects. Representative responses for each of the stimuli are shown in Figs. 2 and 3. Data from subject B2, who could produce voluntary saccadic oscillations, is discussed separately since his oscillations were generally of a slightly lower frequency and higher amplitude than those of the other normal subjects.

Müller paradigm

All normal subjects and the cerebellar patient showed high-frequency conjugate oscillations during combined saccadic-vergence movements. Examples from the cerebellar patient are shown in Figs 2 and 3a; note that the oscillations are most evident on the velocity traces (Figs. 2 and 3a, b) but can be seen on the position traces too (Fig. 2c). The frequency of the oscillations in the cerebellar patient ranged from 26–42 Hz and averaged 35 Hz while the amplitude, measured on position traces, ranged from 0.1–0.3°. He produced saccadic oscillations in about 40% of the trials during both far to near (convergence) and near to far (divergence) gaze shifts. Such oscillations were mostly limited to the horizontal component of eye movement (e.g., Fig. 3a) but were sometimes present in the vertical component as well (e.g., Fig. 2b). The control subjects also produced saccadic oscillations in 20–36% of the trials. An example from subject C1 is shown in Fig. 3c. No significant inter-subject variability was found among the frequencies or the amplitudes recorded in the three control subjects, except for subject B2 for whom the amplitude of the oscillations was significantly greater than for the other control subjects. The frequency of the saccadic oscillations produced by our patient was not significantly different from that of the oscillations produced by the control subjects. The amplitude of his oscillations, however, was significantly greater than that of the oscillations recorded in subjects C1 and B1 ($P < 0.05$).

The subject who could produce conjugate oscillations during voluntary vergence (B2) showed saccadic oscillations during combined vergence-saccade movements with a mean (\pm SD) frequency of 27 ± 4 Hz and amplitude (on position traces) averaging $0.4 \pm 0.1^\circ$. The frequency of these oscillations was significantly lower and the amplitudes significantly larger ($P < 0.01$) than those of the patient and the other control subjects (a representative trial from subject B2 during the Müller paradigm is shown in Fig. 3e).

Overall, these data are similar to findings from ten normal subjects recorded previously, who showed conjugate oscillations during 20–40% of combined saccade-vergence movements (Müller paradigm) (Ramat et al. 1999). The range of mean values for these subjects was

0.2–0.7° in amplitude and 23–33 Hz in frequency. Thus, with respect to the Müller paradigm, the results here are similar to those reported previously.

The percentage of the trials containing oscillations in which a horizontal saccade was present ranged from 60 to 78% for all subjects, including the patient. When preceded by a horizontal saccade, saccadic oscillations occurred during the vergence movement that followed the saccade, starting between 50 and 100 ms after the time of peak velocity of the saccade (e.g., Figs. 3a and 5). Figure 3c shows an example of a response to the Müller paradigm in which there were saccadic oscillations but without any other saccade.

Vertical saccades paradigm

Large (20 and 40°) vertical saccades were elicited in all normal subjects and in the patient. All showed saccadic oscillations in the horizontal plane, which occurred in 30–40% of the trials for all subjects. In this paradigm the oscillations occurred almost exclusively during the vertical saccade. The amplitude and frequency of the oscillations in subjects B1 and C1 were not significantly different from each other and averaged $0.12 \pm 0.03^\circ$ (on position traces) and 32 ± 5 Hz, respectively. An example from subject C1 is shown in Fig. 3d. The patient also showed horizontal saccadic oscillations occurring in about 30% of the trials (Fig. 3b). Oscillations recorded in the patient during the vertical saccade paradigm had the same frequency and amplitude as in the other paradigms and averaged 36 Hz and 0.2° , respectively. These had a significantly larger amplitude ($P < 0.02$) and higher frequency ($P = 0.03$) than those recorded in subjects B1 and C1. Subject B2 showed horizontal oscillations with a mean (\pm SD) frequency of 25 ± 4 Hz and amplitude of $0.5 \pm 0.2^\circ$ (on position traces). These oscillations had significantly lower frequencies and larger amplitudes than those found in the other subjects.

For all subjects and the patient, saccadic oscillations in the horizontal plane began on average 50 ms after the vertical saccade onset and always stopped when the eye came to a stop in the vertical plane Fig. 3b, f.

Midline vergence paradigm

During the midline vergence paradigm we found only five occurrences of oscillations for subject B1. Thus, the data from this subject were discarded from statistical analysis for not meeting the required sample size ($n = 13$, see Methods). Subjects C1, B2 and the patient produced saccadic oscillations in response to the midline vergence paradigm in about 20% of trials, 90% of which were preceded by a small saccade (in the horizontal or the vertical plane).

For subject C1 and for the patient, these oscillations were not significantly different, either in amplitude or frequency, from those recorded during the other paradigms. For subject B2, the oscillations had a smaller

amplitude during midline vergence than during the Müller paradigm or vertical saccades.

As for the Müller paradigm, the oscillations produced by subject B2 during midline vergence were of larger amplitude and lower frequency than those produced by the other normal subjects. Saccadic oscillations were found in significantly fewer trials during midline vergence than in the other paradigms. When saccadic oscillations were found in this paradigm they were preceded by a saccade in either the horizontal or the vertical plane (required in the Lab 1 paradigm) in over 90% of the trials. In the remaining 10% of the trials no saccade was seen (as in Fig. 4c). This raises the question of what happens when the OPN are turned off without a saccadic eye movement.

Blink paradigm

The three normal subjects (B1, B2, C1), but not the patient, were recorded in the pure blink paradigm and all frequently showed saccadic oscillations (>60% of the trials) in the 50–200 ms period following the onset of the blink. The frequency of oscillations was not significantly different ($P > 0.5$) than during the Müller paradigm, though B2 showed significantly smaller amplitude oscillations during blinks ($P < 0.01$). There were no significant differences in the oscillations produced by the different subjects in this paradigm, except for subject B2, who produced oscillations of significantly lower frequency and higher amplitudes. Examples from subjects B1 and B2 are

shown in Fig. 4a and b, respectively. Note that oscillations in these trials were not preceded by a saccade.

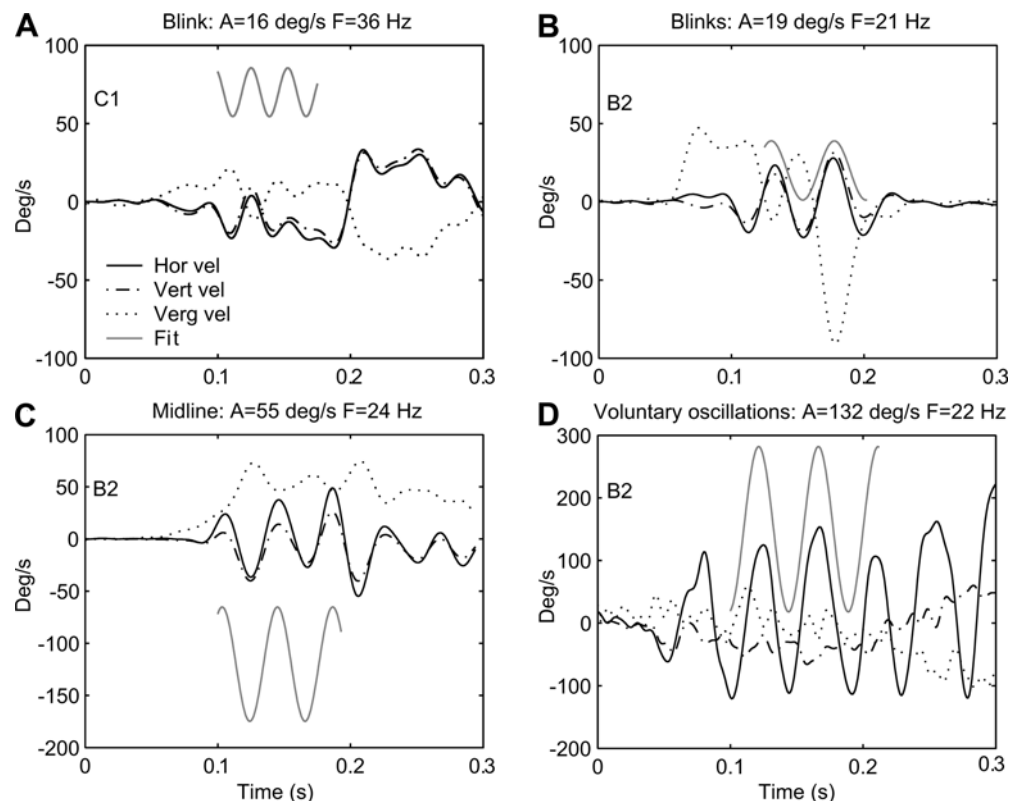
Voluntary conjugate oscillations

Subject B2 could produce conjugate oscillations voluntarily, in association with sustained vergence. He was asked to generate bursts of ‘voluntary nystagmus’ (back-to-back saccades with no intersaccadic interval) [video available] in darkness. The oscillations produced by this subject had a mean (\pm SD) frequency of 24 ± 2 Hz, and amplitude of $0.7 \pm 0.2^\circ$. About 35% of the oscillations were preceded by a small horizontal saccade. The frequency of these oscillations was not statistically different from that of the oscillations generated in the other paradigms, but was lower than those recorded in the other subjects. Amplitudes were significantly larger in this paradigm than in the others. An example of the voluntary oscillations recorded in this subject is shown Fig. 4d.

Comparison of oscillations during different test paradigms for each subject

An overall picture of the frequency characteristics of the oscillations is shown in Fig. 5. Figure 5 shows the histograms of the amplitudes and frequencies of all recorded saccadic oscillations for each subject, except the voluntary oscillations from subject B2, as the amplitudes (velocity traces) of those oscillations were

Fig. 4 a, b Example of high-frequency saccadic oscillations made during the blink paradigm by subject C1 (a) and subject B2 (b). c Example of saccadic oscillations produced during the midline vergence paradigm by subject B2. d Example of saccadic oscillations produced by subject B2 while attempting to produce ‘voluntary nystagmus’. Each panel shows the vertical (dash-dotted) and horizontal (continuous black) version velocity traces; the continuous grey line shows the detrended sinusoidal oscillation. The title of each panel indicates the condition, the amplitude (A) and frequency (F) of the identified sinusoid



often greater than $100^\circ/\text{s}$. Each shade of grey represents one subject, and each column represents the number of oscillations in which the amplitude (measured on velocity traces) or frequency fell within the x-axis bin (cf. figure legend). The plot confirms the similarity of the saccadic oscillations recorded in our subjects in the different conditions and shows how subject B2 represents the lower bound for oscillation frequency and upper bound for amplitude. The overall means and standard deviations including the normal subjects (except B2) and the patient were $0.3 \pm 0.1^\circ$ for amplitude ($25 \pm 13^\circ/\text{s}$ in velocity) and 31 ± 6 Hz for frequency.

For subject B2 and the cerebellar patient saccadic oscillations occurred in a larger percentage of trials across the different conditions, followed by C1 and B1. Overall, the midline vergence paradigm seemed to be least effective in eliciting saccadic oscillations; they were more frequent during blinks and vertical saccades.

To summarize, for all subjects and the patient, the variability of amplitude and frequency found among the different experimental conditions was not greater than that found within one single experimental condition. Thus, we hypothesize that saccadic oscillations are generated by the

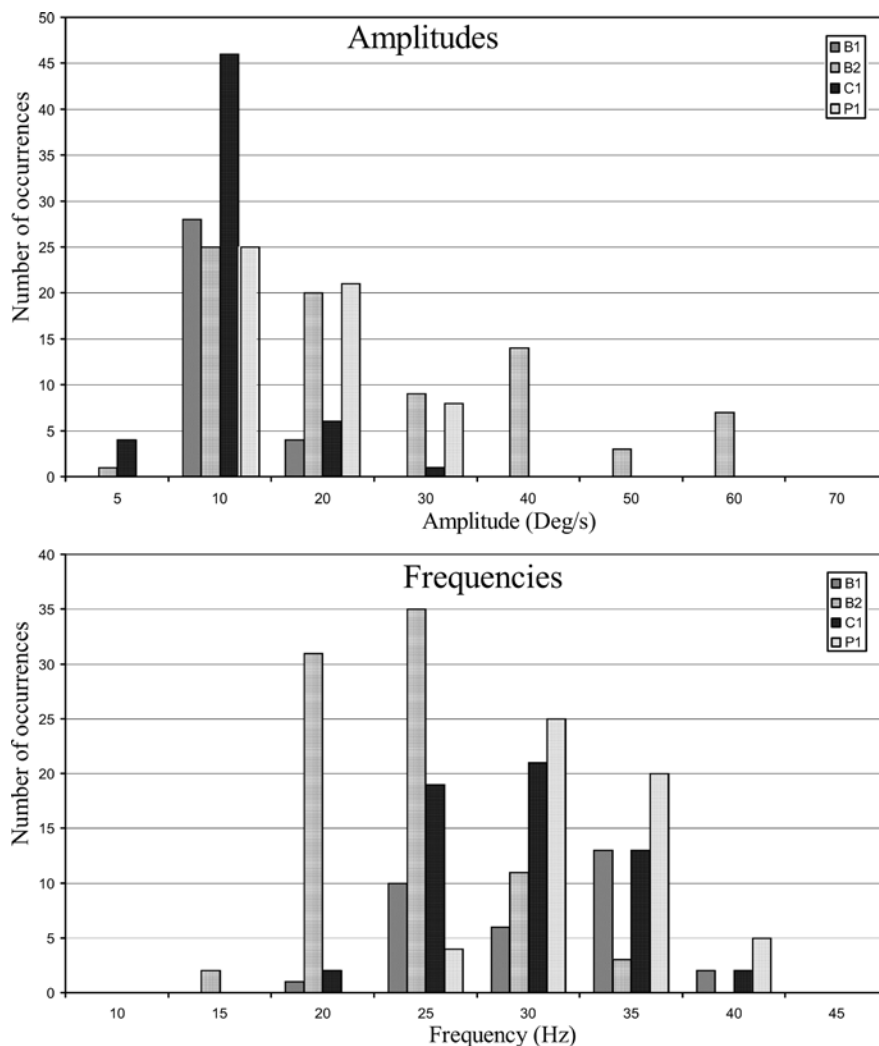
same mechanism in all experimental conditions. Also, the amplitude and frequency characteristics of the saccadic oscillations recorded in the cerebellar patient were not different from those recorded in the other normal subjects. This fact suggests that saccadic oscillations are produced by the same mechanism in the patient and in our normal subjects.

The following sections review the current hypotheses for the mechanism producing saccadic oscillations in the light of our experimental findings and suggest a new, alternative, hypothesis.

Current models

Saccadic oscillations can be explained by a classic control theory model (Fig. 6) that has a negative position feedback loop around a high-gain amplifier (Robinson 1975; Jurgens et al. 1981; Scudder et al. 2002; Sparks 2002). With the desired displacement as an input, this feedback loop generates a burst of innervation proportional to eye velocity and produces a saccade of the correct amplitude and duration. This system can produce saccadic oscilla-

Fig. 5 Distribution of amplitude (measured on velocity traces, *top panel*) and frequency (*bottom panel*) of oscillations recorded in all conditions and all subjects (except B2 in ‘voluntary nystagmus’). Each shade of grey represents one subject. Bar height represents the number of oscillations having amplitude and frequency falling in each interval. Intervals are contiguous so that the lower boundary of one interval is the upper boundary of the preceding interval (e.g., 5–10, 10–20, 20–30 deg/s and so on for amplitudes)



tions because of the high gain of the burst cell and the delay in the feedback pathway (Zee and Robinson 1979). If there is a time delay in the feedback loop, the system oscillates if the phase lag is 180° and the loop gain is at least 1.0 (Zee and Robinson 1979). The duration of the delay in this local feedback loop is the hypothetical mechanism by which the oscillation frequency is modulated (oscillation frequency is inversely related to the delay (τ) by the relationship $F \approx 0.25/\tau$, Zee and Robinson 1979). This *negative feedback model* can oscillate even with no input (unless the loop gain is reduced below one), a condition that may occur if the burst neuron discharge is released from the inhibition of the omnipause neurons.

The range of frequencies of saccadic oscillations reported in normal subjects and patients with flutter or opsoclonus is large: 6–33 Hz (Shults et al. 1977; Ashe et al. 1991; Leigh and Zee 1999; Ramat et al. 1999; Bhidayasiri et al. 2001). To produce such a range of frequencies of oscillations, the *negative feedback model* requires a correspondingly large range of delays ($\tau=36$ to 6 ms). If the feedback signal is local to the brainstem, the source of this six-fold range of delays is not easily understood. Individual synaptic delays are only about 1 ms. Thus, increasing the delay from 6 to 36 ms would require either adding a large number of synapses, or substantially slowing axon conduction. This large range of frequencies of oscillation presents a problem for the classical explanation of saccadic oscillations.

A dual-pathway model has been proposed for the generation of saccadic eye movements that puts the cerebellum in the negative feedback loop responsible for controlling saccadic accuracy (Lefevre et al. 1998; Quaia et al. 1999; Optican and Quaia 2002). It has been proposed that at least part or perhaps all of this feedback pathway goes through the fastigial nucleus (FOR) (Lefevre et al. 1998; Wong et al. 2001). As this path is much longer than an intra-brainstem path, a wider variation of delays might be possible. However, in this model, lesioning the fastigial

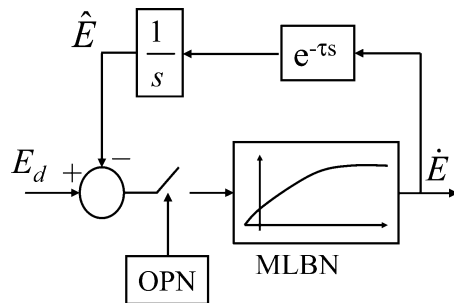


Fig. 6 Classical model of the local position feedback loop for generating the saccade eye velocity command (\dot{E}). Desired eye displacement (E_d) is compared to an efference copy of saccade progress (\hat{E}). The efference copy is obtained by integrating the output of the medium-lead burst neurons (MLBN), which is proportional to eye velocity. The difference between E_d and \hat{E} drives the burst neurons if the OPN are off. If the OPN are turned off and there is no input, the circuit will oscillate with a frequency determined by the delay (τ) in the loop, if the burst neurons have a high enough gain

nucleus opens the negative feedback loop, which produces saccadic hypermetria but prevents saccadic oscillations.

A more detailed examination of the cell types and connections that are known to exist in the brainstem for horizontal movements (Fig. 7) suggests an alternative, novel mechanism for oscillations. In particular, it distributes the role of the burst neurons across two constituent types: excitatory (EBN) and inhibitory (IBN), which are connected across the midline (Strassman et al. 1986b; Büttner-Ennever and Büttner 1992) producing two positive feedback loops. These positive feedback connections provide another source of instability and lead to an alternative model for saccadic oscillations. Common to both models, however, is the hypothesis that a necessary condition for the generation of saccadic oscillations is the inhibition of the OPN.

In the next section, we describe a new model for saccadic oscillation with a mathematical representation of the structures and connections shown in Fig. 7. The model

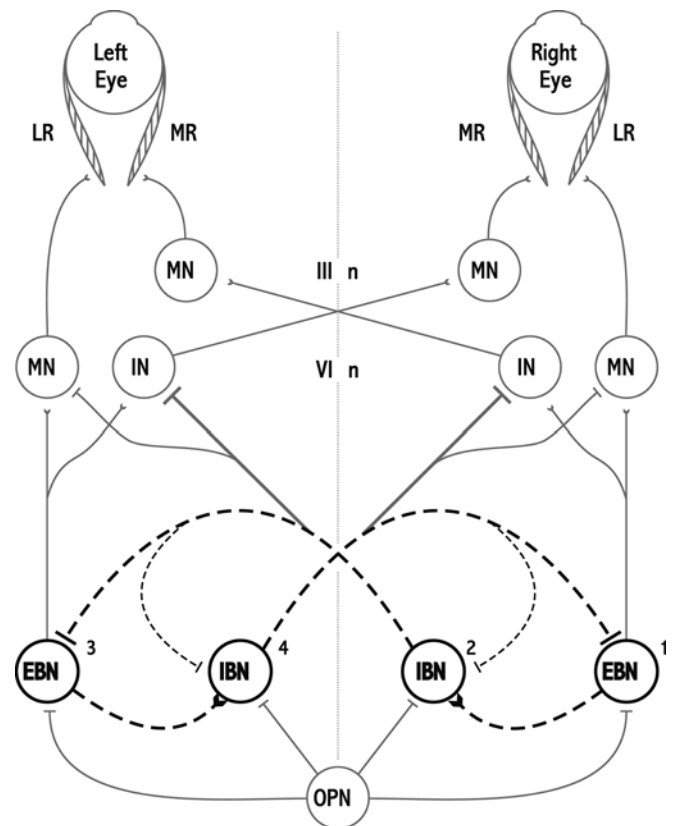


Fig. 7 Details of the brainstem circuit of the dual-pathway model for horizontal saccades. Projections with flat ending are inhibitory, the others excitatory. Saccades require reciprocal innervation to the medial and lateral recti (*ML* and *LR*) of both eyes. The *LR* is driven by the ipsilateral abducens nucleus (*VI n*) motor neurons (*MN*). The *VI n* also contains an interneuron (*IN*) that sends its axon to the contralateral *III n*, which drives the *MR* of the other eye. *EBN* thus provide the drive to the ipsilateral *MN* and *IN*. The *IBN* also project to the ipsilateral *IBN*. The *IBN* provide inhibition to the contralateral *MN* and *IN*. Thus, an *EBN/IBN* pair provides reciprocal innervation. The *IBN* also provide inhibition to the contralateral *EBN* and *IBN*. A consequence of this cross-coupling is that the *EBN/IBN* pairs form a short-latency, positive feedback loop. When *OPN* are active, they prevent this loop from oscillating

is to be considered as a detail of the dual-pathway model of the saccade generator mechanism by Lefèvre et al. 1998. Thus, in its complete form, there would still be a local feedback loop controlling saccadic accuracy, but that would not be the sole mechanism responsible for the oscillations, which can in fact occur even in its absence.

EBN and IBN connectivity

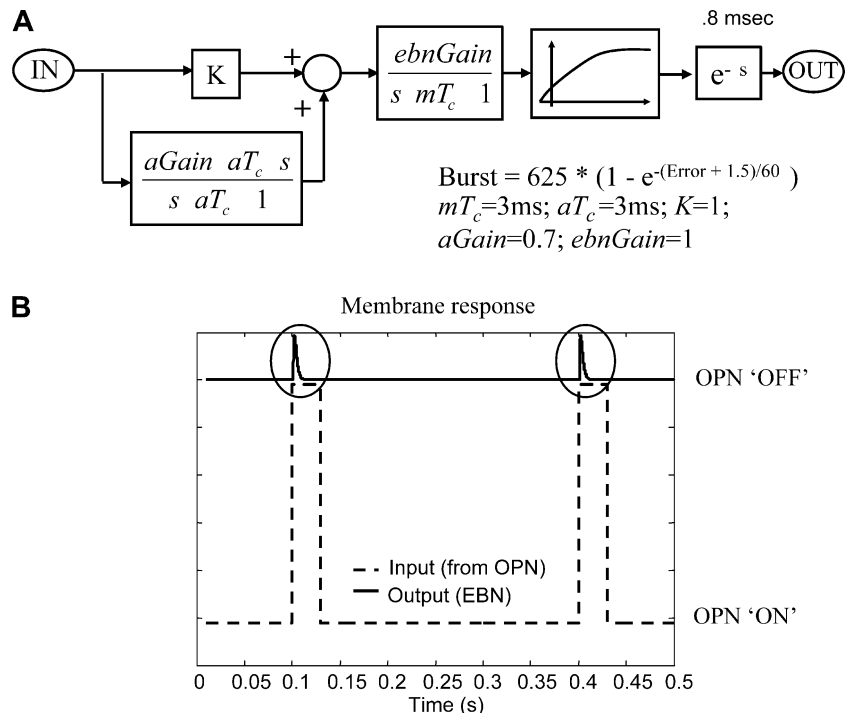
The EBN project to the ipsilateral internuclear and abducens motor neurons, and to the region of the ipsilateral IBN (Strassman et al. 1986a). Axons of the IBN cross the midline and project to the contralateral internuclear and abducens motoneurons, and to the region of the contralateral excitatory and inhibitory burst neurons (Strassman et al. 1986b). The purpose of the crossed projections is to enforce Sherrington’s Law of reciprocal innervation by inhibiting the cells that drive the antagonist motor neurons (Scudder et al. 1988). This ensures that when the saccade begins, only the agonist muscle receives excitation. At the end of the saccade, the model assumes that the opposite IBN are turned on by the ipsilateral fastigial nucleus (not shown in the figure). These opposite IBN in turn send their axons across the midline to inhibit the agonist EBN. This ‘chokes off’ the drive for the saccade and stops the movement (Lefevre et al. 1998; Quaia et al. 1999; Optican and Quaia 2002). Once the movement stops, the OPN resume their discharge and thus inhibit both EBN/IBN pairs.

The coupling of the EBN and IBN across the midline has the additional consequence that one or more short-latency, positive-feedback loops are created (Fig. 7, dashed lines). The shortest loop goes from ipsilateral

IBN to contralateral IBN and back. Neuroanatomical evidence for this projection was found by Strassman et al. (1986b) who reported that “the caudal termination zones of both EBN and IBN cover the region containing the IBN somas.” The longest loop is from the ipsilateral EBN to the ipsilateral IBN, to the contralateral EBN, to the contralateral IBN, and back. When the eyes fixate, these loops are prevented from oscillating by the OPN that inhibit both the IBN and EBN. Note that the complete model published by Scudder (1988, Fig. 8) includes most of the neural structures and connections that are present in the new model proposed here. Notably, the Scudder model suggested the existence of at least two positive feedback loops, a short loop including IBN on both sides of the midline and a longer one including both EBN and IBN. However, the potential of this circuit to oscillate was not explored, possibly because saccadic oscillations are less prominent in monkeys than in humans.

During a horizontal saccade, there is an unbalanced input to EBN, larger in the ipsilateral direction. This causes one side to dominate the other through inhibitory connections, and during the saccade the brainstem circuit does not oscillate. However, at the end of the movement, or during vertical saccades, or during combined saccade-vergence movements, there may be a balanced (or zero) input without OPN inhibition (Zee et al. 1992; Quaia and Optican 1997). Under these circumstances, even a tiny amount of membrane noise or the execution of a small initial saccade may cause the positive feedback circuit to start oscillating. If the synaptic delay is only about 1 ms, however, the frequency of these oscillations would be very high, well above the frequency that the oculomotor plant is capable of responding to (Robinson 1964). Thus, these neural oscillations would look like simultaneous firing on

Fig. 8a, b Burst neuron model allowing postinhibitory rebound and adaptation. **a** The cell membrane contains a low-pass filter (time constant mT_c), and a high-pass filter in a positive feed forward loop. The gain ($aGain$) and time constant (aT_c) of this second high-pass filter determines the amount of post-inhibitory rebound. Burst: output nonlinearity of the burst neurons, see Appendix. **b** Simulation of the neuron model in **a**. The dashed line shows the input to the neuron. The input signal is inhibitory (hyperpolarizing) when it has negative values. Lifting of inhibition is shown for two pulses where the input goes to about 0 V. The neuron output produces post-inhibitory rebound (circled response)



both sides (cf. van Gisbergen et al. 1981), and would not cause eye movements.

Burst neuron membrane properties: post-inhibitory rebound

The model needs a mechanism for slowing down the oscillations that does not depend upon the delays in the coupling loop within the brainstem, and for triggering the oscillations in those conditions in which there is no saccade command (e.g., during blinks). The proposed mechanism is the dynamic properties of the membrane of the neuron. Figure 8a shows the burst neuron model (for both EBN and IBN). The membrane is modeled as a high pass filter that shows adaptation. Thus, the step response of the membrane of the neuron shows an overshoot in both the positive and negative directions. The burst neuron output, however, is determined by the equation describing the saturation element (see Appendix). Thus, the consequence of the adaptation is that at the offset of inhibition there is a rebound that carries the membrane into positive territory, allowing the cell to fire spontaneously (schema in Fig. 8b). Single-unit recordings of EBN show late firing in the previously silent neurons that normally discharge for saccades in the opposite direction (Van Gisbergen et al. 1981). This may be caused by post-inhibitory rebound (PIR). Postinhibitory rebound is a property of some cell types that, at the offset of hyperpolarization, produces a rebound discharge mediated by low-threshold Ca^{++} channels (for a review see Perez-Reyes 2003). Enderle and Engelken (1995) have suggested that this is an important mechanism for generating saccades. Our model depends on PIR to start oscillations when the input to the EBN is *not* imbalanced, i.e., there is no saccade command. For the model to start oscillating without a prior saccade, the OPN must turn off, which in turn produces the post-inhibitory rebound firing (PIR). In the absence of any OPN activity at all (e.g., with a lesion) saccadic oscillations could still occur but only if triggered by a saccade. Finally, the model is relatively insensitive to the exact value of most of its parameters, except for the adaptation time constant (aT_c) and the gain of the EBN (ebnGain).

Model generation of saccadic oscillations

Suppose that the OPN are turned off when there is no horizontal saccade command to the burst neurons. This can occur when subjects make a vertical saccade, a vergence movement, or a blink, as it is believed that OPN are involved in suppressing both saccade and vergence movements (Zee et al. 1992; Mays and Gamlin 1995) and that they turn off during blinks (Hepp et al. 1989; Mays and Morrissette 1995). In our model, the offset of the hyperpolarizing input from the OPN will cause rebound depolarization in both the right and left EBN, which will simultaneously fire a few action potentials. However, any

imbalance in the circuit will allow one side to take over and a periodic oscillation will develop. The numbers in parentheses in the following paragraph refer to those reported in Fig. 7. Suppose the rebound depolarization of the right EBN (1) provides a small output burst that will drive the right IBN (2), which in turn inhibits the left EBN (3). Because of the membrane adaptation, when the burst in the right EBN (1) is over, the left EBN (3) will be disinhibited and its membrane potential will show a rebound depolarization. This rebound will cause the left EBN (3) to burst, which will excite left IBN (4), which, in turn, will lead to inhibition of the original, right EBN (1). When the left EBN (3) shuts off (because it has no input and the PIR is extinguished) the process will be repeated. Thus, the circuit oscillates because of the positive feedback loop around the EBN/IBN pairs on the two sides (two inhibitory projections in one loop make it a positive feedback loop).

In the proposed model, when the drive from the left EBN is over, the right IBN is both disinhibited by the left IBN and excited by the right EBN. Within the right IBN, this excitation is amplified by the rebound properties of the neuron so that the input to their saturation element (the block labeled “burst” in Fig. 8a) is carried to large positive values, thus causing these neurons to fire at their saturation level. The input to the EBN cells, instead, never reaches positive values when the circuit is not driven to produce a saccade. In fact, when a driving command is absent the only possible inputs to EBN are inhibitory; thus in these conditions these cells are either inhibited or disinhibited, but never excited. Any positive input to the output saturation of the EBN is thus due uniquely to PIR and can be easily modulated by the membrane gain parameter, ebnGain, so as to fall into the approximately linear part of the saturation element of the neuron. Such modulation does not affect the duration of the rebound burst (and therefore the circuit oscillation frequency) but only its intensity (the maximum firing rate of the rebound, and therefore the amplitude of the oscillation). Our model would thus predict that the IBN would always begin firing at their saturation level, while the EBN could show a modulation of their initial firing rates during oscillations. Simulations based on this model (see below) show that the frequency of oscillation is mainly controlled by the EBN adaptation time constant, while the amplitude is controlled by the EBN adaptation time constant and the membrane gain.

When a similar EBN/IBN organization was first suggested by Scudder (1988) for monkeys, the author did not report oscillations in the behavior of his model, presumably because of the low gain used for the IBN to IBN projections (0.15, a value too low to inhibit the target neurons). There is relatively little data on the occurrence and characteristics of saccadic oscillations in monkeys (e.g., Fig. 11b, *left panel, top trace* in Sylvestre et al. 2002).

Model simulations

Next we present model simulations of the saccadic oscillations for the normal subjects and the cerebellar patient in paradigms occurring either with (vertical saccades, saccade-vergence) or without an associated saccade ('voluntary nystagmus', blinks and pure vergence). All simulations were performed using a leaky integrator and two-pole plant. The slowest pole of the plant (time constant of 200 ms) is compensated by the zero in the leaky integrator (Chun and Robinson 1978) so that only the second pole of the plant (time constant of 15 ms) needs to be considered for producing the ocular motor output. The critical parameters that determine the characteristics of the oscillations are the membrane adaptation time constant, which accounts for the adaptation properties of PIR, and the membrane gain, which accounts for both the probability and the overall intensity of PIR across the population of neurons. As the time constant for the adaptation changes, the amplitude and frequency of the oscillation also changes (Fig. 9a and b, respectively). Varying the membrane gain of the burst neurons but not the adaptation time constant has only a small effect on the oscillation frequency (Fig. 9b) but considerably modulates the oscillation amplitude (velocity amplitude shown in Fig. 9a). The ability to modulate the amplitude independently of the frequency is reflected in the experimental data, such as that presented in Fig. 4b–d in which oscillations produced by the same subject can have similar frequencies but different amplitudes.

Varying the adaptation time constant over a tenfold range from 3 to 30 ms causes the frequency to change from about 40 to about 6 Hz (depending also on the value of the *ebnGain*). In our simulations the adaptation time constant of the IBN was set to the same value as that of the

EBN. Varying the adaptation time constant of the IBN independently from that of the EBN did not have substantial effects on either the amplitude or frequency of the oscillations produced by the model. In our lumped model the characteristics of PIR adaptation are determined by the membrane adaptation time constant (aT_c). The overall probability of PIR over a population of neurons and the resulting intensity modulation are represented by the gain of the membrane of the burst neuron (*ebnGain*).

Examples of the oscillations generated by our model, without the cerebellar negative feedback loop, are shown in Fig. 10. Figure 10b presents oscillations obtained with three different combinations of gain and time constant of the membrane simulating oscillations following an initial horizontal saccade. A saccadic command of a predetermined duration was given as the input to the model, causing inhibition of the OPN, which are then kept off until 200 ms later. At the end of the saccade, the oscillations settle in. Figure 10a shows simulations of oscillations that are not preceded by an initial saccade and that are sparked only by post inhibitory rebound due to the OPN being shut off (after 25 ms) and then kept silent until 200 ms later. Also, the occasional drift of the oscillations as well as the changing frequency and amplitude can be simulated with small imbalances between the right and left parts of the circuit, and by allowing small (e.g., 0.1 ms) on-line variations of the membrane characteristics. The latter could be the result of biological noise, which could affect both the PIR characteristics of single neurons (which could depend on ionic and cationic currents, the duration and intensity of the preceding hyperpolarization and several types of neurotransmitters) and whether or not an individual burst neuron will show PIR. Thus, the net population discharge could vary over time.

Fig. 9a, b Simulation of saccadic oscillations. The velocity amplitude (a) and frequency (b) of the oscillations as a function of the adaptation time constant and burst neurons gain. Note that the view point is different in a and panel b. Model parameters for simulations are reported in Table 1

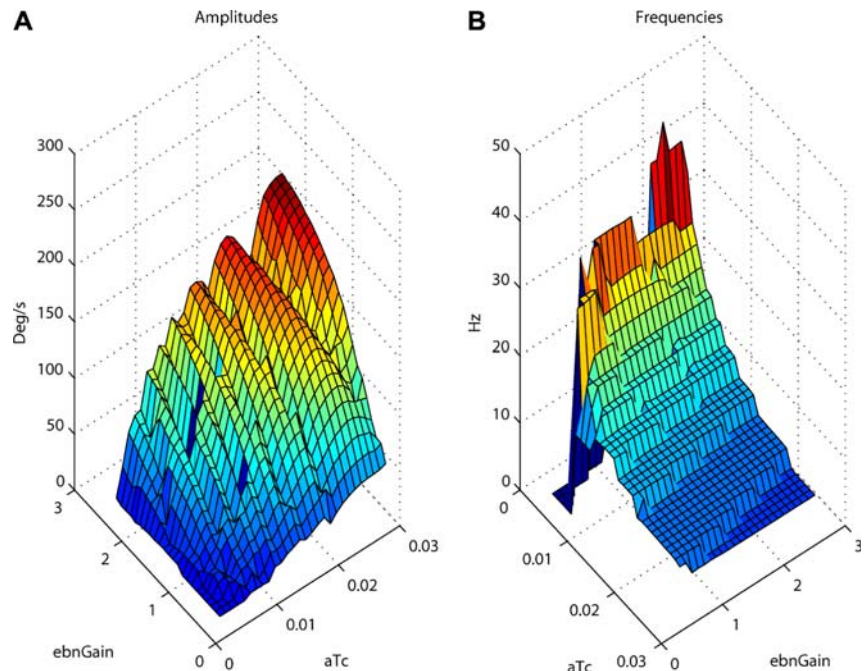
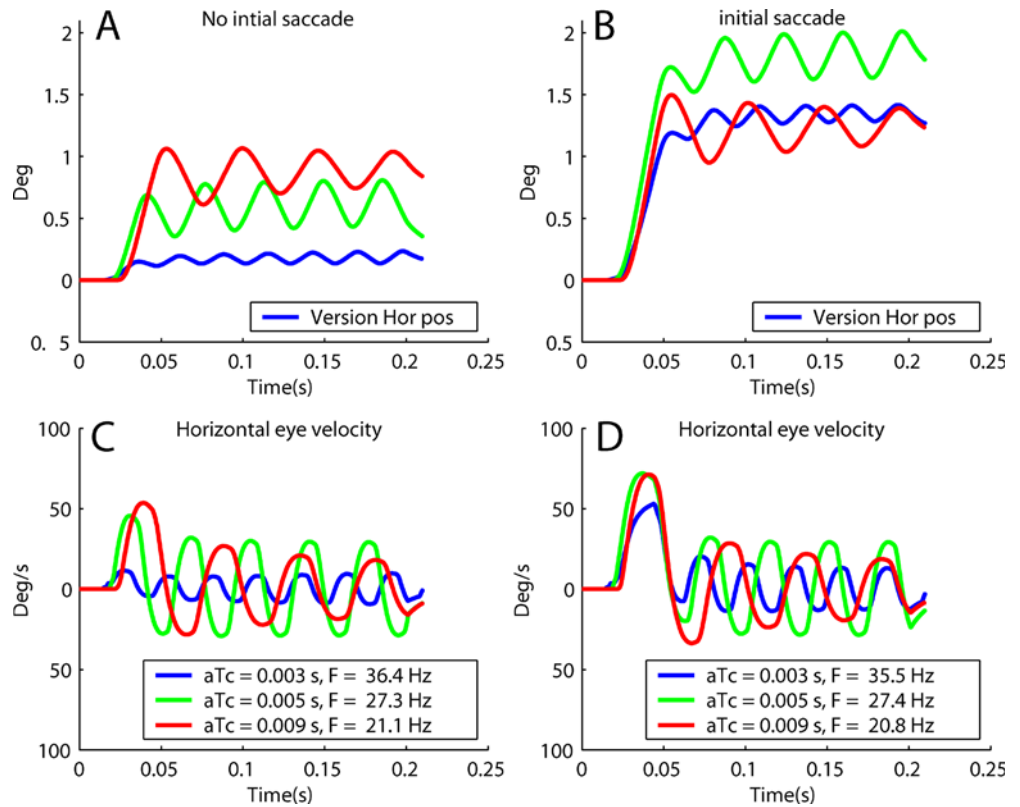


Fig. 10a-d Simulations of saccadic oscillations for different aT_c values obtained with the model without a local feedback loop. **a, c** Eye position and eye velocity of saccadic oscillations produced without a preceding saccade. **b, d** Eye position and velocity traces of saccadic oscillations preceded by a 1° saccade. The behavior of the OPN is the same in both sets of simulations: OPN turn off at 20 ms and turn on at 200 ms, $ebnGain=0.4$



We also added the ‘classical’ local negative feedback loop (Fig. 6) to our model, using different delays, to simulate the response with a complete saccade generator. The amplitude and frequency characteristics of saccadic

oscillations generated by the complete model are only marginally affected by the delay along the negative feedback loop. We simulated the model with different (from 2 to 20 ms) values of the delay along the loop and

Fig. 11a-d Simulations of saccadic oscillations obtained with our model to which the classical negative local feedback loop was added. The same combinations of parameter values shown in Fig. 10 were used. **a, c** Eye position and eye velocity of saccadic oscillations produced without a preceding saccade. **b, d** Eye position and velocity traces of saccadic oscillations preceded by a 1° saccade. The behavior of the OPN is the same in both sets of simulations: OPN turn off at 20 ms and turn on at 200 ms, $ebnGain=0.4$

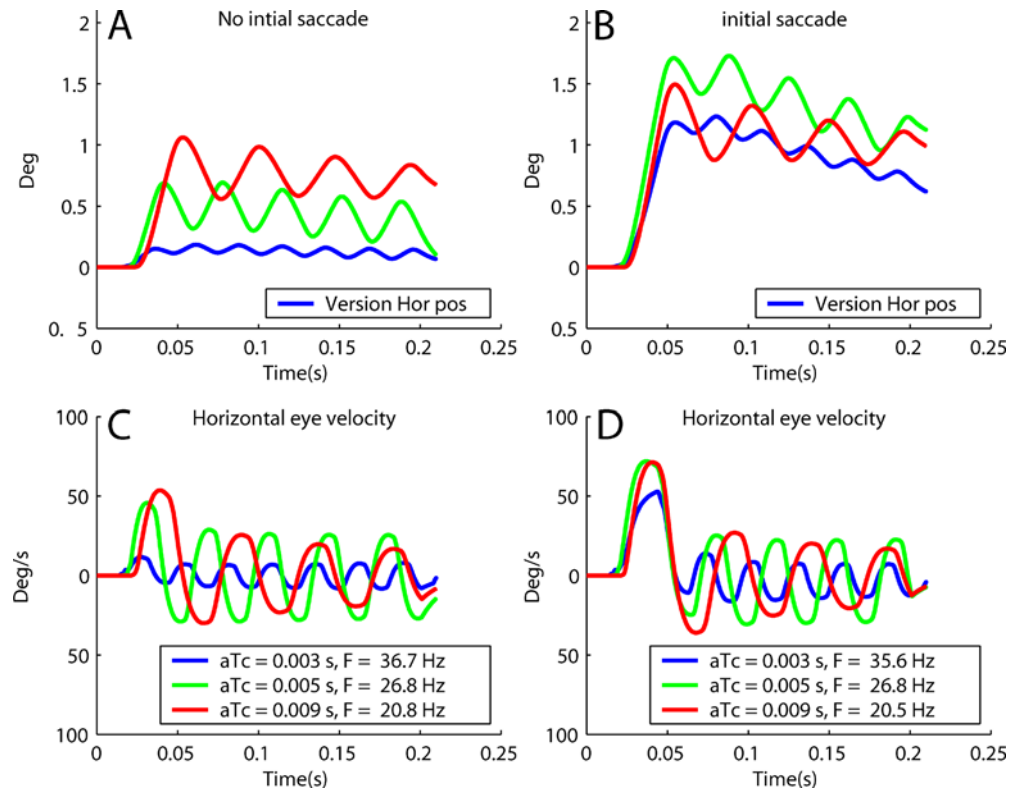
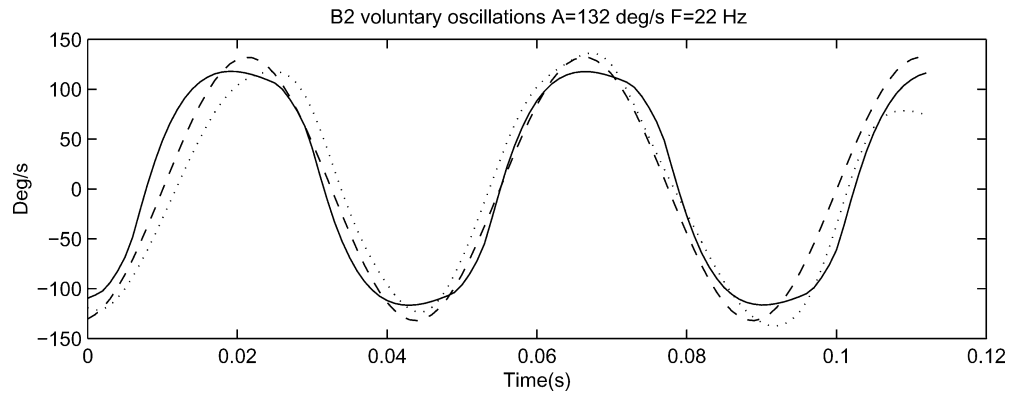


Fig. 12 Simulation of experimental data from subject B2 (Fig. 7a) who could produce voluntary conjugate oscillations. *Dotted trace*: detrended eye velocity. *Dashed trace*: sinusoidal fit to the dotted trace. *Continuous trace*: model simulation



found that the sensitivity of the model to such changes peaked for a delay of 10 ms. Even so, that delay caused less than a 5% reduction in the frequency of the oscillations (Fig. 11) compared with those generated by the model without the negative feedback when using the same membrane parameters as in Fig. 10. The effect of the negative local feedback loop can be appreciated in the position traces (panel b) of the simulations of oscillations following a saccade. The baseline of the oscillation decays toward the reference position with a time constant on the order of 100 ms. The simulations of oscillations generated by the complete model without an initial saccade (panel a and c) differ only slightly in their amplitude and frequency from those obtained without the local feedback loop.

Examples of simulations of voluntarily induced saccadic oscillations are shown in Fig. 12, in which the conjugate velocity trace from the trial shown in Fig. 4d is analyzed. The figure shows the detrended oscillation together with the sinusoidal fit. The oscillations had a frequency of 22 Hz and amplitude of 132°/s. Also shown are simulations of the oscillations when setting $aT_c = 4.4$ ms and $ebnGain = 0.75$. Note that all experimental conditions have the inhibition of the OPN in common. Our model focuses on the mechanism inducing the oscillations in these different paradigms. The model does not and was not meant to simulate the complete ocular motor responses to the different paradigms.

In summary, the model simulated the oscillations successfully for all subjects in all experimental conditions, producing oscillations that were within 1 Hz and 2°/s amplitude of those actually recorded. For a given value of the $ebnGain$ parameter, the differences between the subject able to produce voluntary oscillations and the other control subjects and the patient were accounted for by an increase of the aT_c parameter. The aT_c parameter averaged about 3 ms in all subjects, with the exception of subject B2, for whom the aT_c parameter ranged from 4 to 8 ms.

Discussion

The experiments presented here dealt with three major questions:

- Can saccadic oscillations comparable to those previously reported in response to the Müller paradigm be observed during other experimental paradigms in which OPN are inhibited?
- Does a patient who has a bilateral fastigial nuclei lesion produce saccadic oscillations with similar amplitude and frequency to those of normal subjects? This finding would be at odds with the recent hypotheses in which saccadic oscillations are attributed to a relay of the local feedback through the fastigial nuclei.
- Can we explain the generation of saccadic oscillations using a new model that does not rely upon the integrity of the fastigial nuclei?

Experimental observations of saccadic oscillations under a variety of conditions

A previous study reported saccadic oscillations elicited in normal subjects by combined saccade-vergence movements (Ramat et al. 1999). It was hypothesized that saccadic oscillations occurred during combined saccade-vergence movements because the saccadic system is not inhibited (i.e., the OPN are silent) during the vergence movement that follows the saccade (Ramat et al. 1999). We thus further investigated whether saccadic oscillations similar to those previously found in response to the Müller paradigm could also be observed during other experimental paradigms causing the inhibition of the OPN. Single unit recording data shows that omnidirectional pause neurons (OPN) are shut off during saccades in all directions (Keller 1974), and during blinks (Hepp et al. 1989; Mays and Morriss 1995). Furthermore, behavioral and electrophysiological evidence suggests that OPN are inhibited by vergence (Mays and Gamlin 1995; Scudder et al. 2002; Busettini and Mays 2003).

Thus, we recorded the responses of normal subjects in different experimental conditions causing the inhibition of the OPN, including conjugate vertical saccades, blinks, combined saccade-vergence movements, pure vergence and ‘voluntary nystagmus’, in order to determine whether saccadic oscillations aroused even in these conditions.

We found that normal subjects occasionally produced saccadic oscillations during all these experimental condi-

tions and that the characteristics of the oscillations were similar across conditions.

In our recordings, the dependency of saccadic oscillations upon the behavior of the OPN was most evident during the vertical saccades paradigm, in which the lack of any horizontal eye movement requirement emphasized the synchronization of the end of the oscillations with the end of the vertical saccade (Fig. 3b, d, f). Responses from the vertical saccade paradigm clearly show that once the OPN are off, although there is no saccadic command to the horizontal burst neurons, horizontal oscillations can arise spontaneously. Saccadic oscillations were found also in trials in which no appreciable saccade (in any direction) was recorded (Figs. 3c and 4), thus suggesting that other mechanisms besides saccades, including blinks and possibly vergence can be associated with turning off or abruptly reducing the discharge of the OPN.

Experimental observations of saccadic oscillations in a patient with a bilateral fastigial nuclei lesion

Our patient with a midline cerebellar lesion showed bilateral saccadic hypermetria, consistent with experimental, bilateral inactivation of the fastigial nucleus (Robinson et al. 1993). His MRI shows bilateral involvement of the fastigial nucleus, while his saccadic hypermetria indicates impaired feedback control of saccade trajectory. Nevertheless, he developed the same high-frequency, conjugate oscillations during saccade-vergence movements as do normal subjects. Thus, why are there high-frequency saccadic oscillations in this patient without feedback through the fastigial nucleus?

The model originally proposed to account for saccadic oscillations by Zee and Robinson (1979) has been updated by Wong and colleagues (2001). They adapted Dean's model (Dean 1995) of the cerebellar contribution to saccades to explain opsoclonus (large amplitude, pathological saccadic oscillations). They noted that opsoclonus can occur even when the OPN are not damaged, and thus they proposed that a delayed, high-gain, high-pass feedback loop through the fastigial nucleus produced the oscillations. In both models (Zee and Robinson 1979; Wong et al. 2001), the oscillations occur because the OPN are not inhibiting the EBN. Then, the high gain in the negative feedback loop causes the oscillations. There are two problems with these models. First, they do not explain the wide range in time delays required to produce the six-fold range of frequencies observed in saccadic oscillations (Ashe et al. 1991; Leigh and Zee 1999; Ramat et al. 1999; Bhidayasiri et al. 2001). Second, the saccadic oscillations shown by the cerebellar patient during saccade-vergence cannot be explained by a fastigial feedback-pathway mechanism since presumably the lesion interrupted the feedback loop. On the other hand, even if we hypothesize that some auxiliary pathway might have been recruited to close the feedback loop in the patient, such a pathway would likely contain an even longer delay, producing much lower frequency oscillations. In fact, the oscillations

in the cerebellar patient were in the same range as normal subjects with an intact feedback loop.

A new model for saccadic oscillations based upon EBN-IBN coupling

Here we have developed a new model to account for saccadic oscillations in both normal subjects and a patient with a cerebellar lesion. We suggest our model as an alternative mechanism to the classic local feedback loop model (Zee and Robinson 1979) which simulates the wide range of frequency of oscillations reported in the literature (6–33 Hz) but requires large, physiologically unlikely, changes in transmission time in the feedback loop. In the new model the oscillations occur in the absence of the traditional local feedback loop, which is a requirement to simulate the findings in the cerebellar patient with the fastigial nucleus lesion, if the local feedback loop is indeed mediated by the fastigial nucleus (Lefevre et al. 1998; Wong et al. 2001). Moreover, the range of frequency and amplitude of the oscillations can be reproduced with minimal variations of the membrane properties, which appears to be more plausible than the relatively large variation of a delay along a neural pathway.

Our simulations suggest that high-frequency saccadic oscillations in normal subjects, and perhaps some pathological oscillations as well, may be generated by positive-feedback connections between pontine inhibitory and excitatory burst neurons, and occur when omnipause neurons are inhibited. The mechanism of oscillation is the coupling of the IBN, and the membrane adaptation that gives rise to post-inhibitory rebound in the EBN and IBN. Our model relies on the ability of the burst neurons to produce postinhibitory rebound firing, an intrinsic property that has been recently recognized in different populations of neurons in the cerebellum, such as the deep cerebellar nuclei (Aizenman and Linden 1999), in the brainstem, such as the vestibular nuclei (Sekirnjak and du Lac 2002), and in other neural structures (Perez-Reyes 2003). In the medial vestibular nuclei, for instance, it has been shown that large, multipolar neurons tend to produce post-inhibitory rebound discharge. Depending on the neuron and on the characteristics of the preceding hyperpolarization, these neurons fire one or more spikes upon release of inhibition. Neurons in the medial vestibular nuclei (MVN) that exhibit such behavior are characterized by a pronounced adaptation (exponential decay) of the firing frequency of the rebound depolarization (Sekirnjak and du Lac 2002). Neurons with similar behavior, with low-voltage activated calcium channels (T-type), were also identified within the thalamus. Because they are interconnected by excitatory-inhibitory projections, it has been hypothesized that they are responsible for the rhythmic behavior found in thalamic firing patterns (Huguenard 1998; Huntsman et al. 1999; Sohal et al. 2000; Jacobsen et al. 2001) Thus, post-inhibitory rebound is an intrinsic property of different classes of neurons and has been shown to display varying characteristics in its

probability, and its intensity and duration, depending on both the instantaneous inputs to the cell and on its history (see Perez-Reyes (2003) for a review). Our model, like that suggested by Enderle and Engelken (1995), postulates that EBN and IBN neurons (or a subset of these neurons) may produce post-inhibitory rebound firing. Note that we are formulating an hypothesis on the properties of burst neurons based on analogies with other neurons of the central nervous system. Although there currently are no data proving such assumption, our hypothesis should guide further experiments investigating the properties of burst neurons. In our model saccadic oscillations are produced whenever the inhibition exerted by the OPN is lifted. In the absence of a saccade-drive signal to the brainstem, the cross-coupled circuit of excitatory and inhibitory burst neurons (EBN and IBN) (Fig. 7) starts oscillating, sparked by postinhibitory rebound discharge. Postinhibitory rebound discharge is responsible for the initiation of oscillations—in conditions in which no initial saccade is produced—and for controlling the characteristics of the oscillations.

In our model the coupling of EBN and IBN, and post-inhibitory rebound firing gives rise to oscillations that depend on the adaptation time constant of the membrane of the burst neurons, which controls the duration of post-inhibitory rebound, and thus both the frequency and amplitude of the oscillations. The actual values of the time constants of EBN and IBN membranes and their moment-to-moment variability have not been reported but in other systems inactivation time constants for calcium channels are ~ 10 ms, whereas potassium and sodium channels are shorter (Perez-Reyes 2003). Biophysical studies of EBN and IBN membrane characteristics are needed to establish time constants of channel inactivation in these unusual neurons. The oscillations also depend on the gain of the membrane, which controls the intensity of the rebound, and thus primarily affects the amplitude of the oscillations (Fig. 9). Varying the time constant from 4 to 20 ms causes the frequency to change from 37 to 5 Hz. This includes the entire range of oscillation frequencies observed across subjects and patients both in the literature and in this study. Furthermore, the range of variability in the time constant of adaptation proposed here seems physiologically more reasonable than such a large variability in neuronal delays. A delay can only change because the path changes (thereby incorporating more or fewer synapses) or because the conduction velocity of the neurons changes. Neither is likely to happen instantaneously in normal subjects, precluding an explanation for the within subject variability shown by our subjects. Considering the 95% confidence interval for the frequency parameters of the sinusoidal fit, every subject showed about 10 Hz of variability in oscillation frequency within the same experimental condition, which would require a corresponding variation in the feedback delay of about 3 ms. The postinhibitory rebound properties of neurons have been shown to depend upon a number of factors as ionic and cationic currents and neurotransmitter concentrations (cf. Aizenman and Linden 1999, Sekirnjak and du Lac 2002). Thus, postinhibitory

rebound is likely to be affected by biological noise both at the level of individual neurons and in terms of probability of producing post-inhibitory rebound firing over the entire population of burst neurons. These effects, which in our lumped model are represented at the level of the membrane properties of the single neuron that we modeled, are a more likely source of variability for the frequency of the resulting oscillations than changes in the delay along the local feedback loop. In fact, our model oscillates with similar dynamics both with and without a local feedback loop, and is relatively insensitive to the duration of the delay (Figs. 10 and 11).

Our simulations do not address what would be the effect of disinhibition of only a portion of the burst neuron pool on saccadic oscillations. This may account for the fact that saccadic oscillations are less frequent in the midline vergence paradigm.

In agreement with the experimental findings of Soetedjo and colleagues (2002), our model does not predict oscillations following the inactivation of the OPN as burst neurons would not produce PIR when the OPN are continuously off. For a neuron to show PIR, the OPN must be *turned* off, thus lifting the inhibition on the burst neurons. The model also suggests an explanation for oscillations being more common in humans than in monkeys (Busetini and Mays 2003): the higher gain of the burst neurons in monkeys ($B_m \approx 1,000^\circ/s$ in the equation for the burst neuron nonlinearity, see Appendix) causes the neurons on both sides of the midline to fire simultaneously for a longer period of time before the oscillations emerge. In order for oscillations to develop earlier in the monkey, the model needs a larger imbalance in the inhibitory projections (ibnRL and ibnLR, see Table 2).

In summary, we have demonstrated saccadic oscillations with similar characteristics in a variety of experimental paradigms in a group of normal subjects. Oscillations with the same amplitude and frequency characteristics were found in a patient with bilateral lesions of the fastigial nuclei. We suggest that the mechanism is the post-inhibitory rebound of locally cross-coupled inhibitory and excitatory burst neurons in the brainstem. Such a mechanism for the generation of oscillations by the brainstem reticular formation might account for oscillatory behavior in other motor systems.

Table 2 Model parameters used for the full range of simulations shown in Fig. 9

Parameter	Value
aT_c	0.003–0.030 s
ebnGain	0.3–2.5
aGain	1.2
mT_c	0.003 s
ibnLR	1.8
ibnRL	2.0
synDelay	0.0008 s
B_m	$600^\circ/s$
e_0	-1.5°
B	60°

The head control (cephalomotor) system would be a good candidate since it may have an analogous premotor organization and also close links to the saccadic eye movement control system. A similar network of excitatory and inhibitory neurons arranged in positive feedback was suggested for the generation of the rhythmic discharging governing locomotion in frog embryos (Roberts and Tunstall 1990). Our model thus emphasizes the fundamental role that the specific properties of the cells involved may have in the production of a motor behavior. Finally, although the focus of our paper has been horizontal saccades generated by the saccadic system, the model might also be extended to account for the 3-D saccadic oscillations of opsoclonus (Leigh and Zee 1999).

Acknowledgements Supported by USPHS grant EY06717, the Office of Research and Development, Medical Research Service, Department of Veterans Affairs, and the Evenor Armington Fund (to R.J. Leigh), USPHS grant EY01849 to D.S. Zee. David Linden provided helpful discussion. Dr. Stefano Ramat was supported by the Robert M. and Annetta J. Coffelt Endowment for PSP research. The authors are grateful to Jeffrey Somers for assistance with experiments.

Appendix

The model of coupled burst neurons was simulated in Simulink/Matlab. The structure of the model included OPN and two EBN/IBN pairs, connected as shown in Fig. 7. Individual neurons contained an adaptation element (as in Fig. 8a) and a synaptic delay (τ). Values for the cross-coupling coefficients and other dynamic properties are given in Table 2. The final common path (i.e., neural integrator and orbital tissues) was modeled with an integrator and one uncompensated, single-pole filter (time constant Teye).

The medium lead burst neurons were represented by bilateral pairs of inhibitory and excitatory burst neurons. Both EBN and IBN were modeled like the OPN, except that a soft-saturating nonlinearity was added to the output. The equation for this element comes from Zee and Robinson (1979):

$$B(e) = \begin{cases} B_m(1 - e^{-(e-e_0)/b}), & e > e_0 \\ 0, & e \leq e_0 \end{cases} \quad (1)$$

This element was added to reduce the harmonic distortion in the saccadic oscillations that was present when a hard saturation element was used. In this equation the input variable e represents motor error for the Robinson model, whereas in our model e represents an input in terms of the frequency of discharge rate, which is related to eye velocity. The values for the parameters in these equations were therefore derived from those in the original model and scaled to reflect the different input variables (cf. Table 2). The EBN and IBN were reciprocally coupled across the midline. EBN projected to ipsilateral IBN with a gain of 1.0. IBN projected to

contralateral EBN with a gain of 1.0 and to contralateral IBN with a gain of either ibnLR (Left to Right side) or ibnRL (Right to Left side). These gain values were not perfectly symmetric, to ensure that the system would start oscillating as soon as the OPN shut off. When equal gains were used, the system was quasi-stable, and would only begin to oscillate after a few hundred milliseconds.

References

- Aizenman CD, Linden DJ (1999) Regulation of the rebound depolarization and spontaneous firing patterns of deep nuclear neurons in slices of rat cerebellum. *J Neurophysiol* 82:1697–1709
- Ashe J, Hain TC, Zee DS, Schatz NJ (1991) Microsaccadic flutter. *Brain* 114:461–472
- Bergamin O, Zee DS, Roberts DC, Landau K, Lasker AG, Straumann D (2001) Three-dimensional Hess screen test with binocular dual search coils in a three-field magnetic system. *Invest Ophthalmol Vis Sci* 42:660–667
- Bhidayasiri R, Somers JT, Kim JI, Ramat S, Nayak S, Bokil HS, Leigh RJ (2001) Ocular oscillations induced by shifts of the direction and depth of visual fixation. *Ann Neurol* 49:24–28
- Busettini C, Mays LE (2003) Pontine omnipause activity during conjugate and disconjugate eye movements in macaques. *J Neurophysiol* 90:3838–3853
- Büttner-Ennever JA, Büttner U (1992) Neuroanatomy of the ocular motor pathways. *Baillieres Clin Neurol* 1:263–287
- Büttner-Ennever JA, Cohen B, Pause M, Fries W (1988) Raphe nucleus of the pons containing omnipause neurons of the oculomotor system in the monkey, and its homologue in man. *J Comp Neurol* 267:307–321
- Chun KS, Robinson DA (1978) A model of quick phase generation in the vestibuloocular reflex. *Biol Cybern* 28:209–221
- Collewijn H, van der SJ, Steinman RM (1985) Human eye movements associated with blinks and prolonged eyelid closure. *J Neurophysiol* 54:11–27
- Dean P (1995) Modelling the role of the cerebellar fastigial nuclei in producing accurate saccades: the importance of burst timing. *Neuroscience* 68:1059–1077
- Duvernoy HM (1995) The human brain stem and the cerebellum. Springer, New York
- Efron B, Tibshirani RJ (1993) An introduction to the bootstrap. Chapman and Hall, New York
- Enderle JD, Engelken EJ (1995) Simulation of oculomotor post-inhibitory rebound burst firing using a Hodgkin-Huxley model of a neuron. *Biomed Sci Instrum* 31:53–58
- Evinger C, Kaneko CR, Fuchs AF (1982) Activity of omnipause neurons in alert cats during saccadic eye movements and visual stimuli. *J Neurophysiol* 47:827–844
- Hain TC, Zee DS, Mordess M (1986) Blink-induced saccadic oscillations. *Ann Neurol* 19:299–301
- Hepp K, Henn V, Vilis T, Cohen B (1989) Brainstem regions related to saccade generation. *Rev Oculomot Res* 3:105–212
- Horn AK, Büttner-Ennever JA, Suzuki Y, Henn V (1995) Histological identification of premotor neurons for horizontal saccades in monkey and man by parvalbumin immunostaining. *J Comp Neurol* 359:350–363
- Hotson JR (1984) Convergence-initiated voluntary flutter: a normal intrinsic capability in man. *Brain Res* 294:299–304
- Huguenard JR (1998) Low-voltage-activated (T-type) calcium-channel genes identified. *Trends Neurosci* 21:451–452
- Huntsman MM, Porcello DM, Homanics GE, DeLorey TM, Huguenard JR (1999) Reciprocal inhibitory connections and network synchrony in the mammalian thalamus. *Science* 283:541–543
- Jacobsen RB, Ulrich D, Huguenard JR (2001) GABA(B) and NMDA receptors contribute to spindle-like oscillations in rat thalamus in vitro. *J Neurophysiol* 86:1365–1375

- Jurgens R, Becker W, Kornhuber HH (1981) Natural and drug-induced variations of velocity and duration of human saccadic eye movements: evidence for a control of the neural pulse generator by local feedback. *Biol Cybern* 39:87–96
- Keller EL (1974) Participation of medial pontine reticular formation in eye movement generation in monkey. *J Neurophysiol* 37:316–332
- Lefèvre P, Quaia C, Optican LM (1998) Distributed model of control of saccades by superior colliculus and cerebellum. *Neural Netw* 11:1175–1190
- Leigh RJ, Zee DS (1999) *The neurology of eye movements*. Oxford University Press
- Mays LE, Gamlin PD (1995) Neuronal circuitry controlling the near response. *Curr Opin Neurobiol* 5:763–768
- Mays LE, Morriss DW (1995) Electrical stimulation of the pontine omnipause area inhibits eye blink. *J Am Optom Assoc* 66:419–422
- Optican LM, Quaia C (2002) Distributed model of collicular and cerebellar function during saccades. *Ann N Y Acad Sci* 956:164–177
- Perez-Reyes E (2003) Molecular physiology of low-voltage-activated t-type calcium channels. *Physiol Rev* 83:117–161
- Quaia C, Optican LM (1997) Model with distributed vectorial premotor bursters accounts for the component stretching of oblique saccades. *J Neurophysiol* 78:1120–1134
- Quaia C, Lefevre P, Optican LM (1999) Model of the control of saccades by superior colliculus and cerebellum. *J Neurophysiol* 82:999–1018
- Ramat S, Somers JT, Das VE, Leigh RJ (1999) Conjugate ocular oscillations during shifts of the direction and depth of visual fixation. *Invest Ophthalmol Vis Sci* 40:1681–1686
- Roberts A, Tunstall MJ (1990) Mutual re-excitation with post-inhibitory rebound: a simulation study on the mechanisms for locomotor rhythm generation in the spinal cord of xenopus embryos. *Eur J Neurosci* 2:11–23
- Robinson DA (1964) The mechanics of human saccadic eye movement. *J Physiol (London)* 174:245–264
- Robinson DA (1975) Oculomotor control signals. In: Lennerstrand G, Bach-y-Rita P (eds) *Basic mechanisms of ocular motility and their clinical implications*. Pergamon Press, Oxford, pp 337–374
- Robinson FR, Fuchs AF (2001) The role of the cerebellum in voluntary eye movements. *Annu Rev Neurosci* 24:981–1004
- Robinson DA, Keller EL (1972) The behavior of eye movement motoneurons in the alert monkey. *Bibl Ophthalmol* 82:7–16
- Robinson FR, Straube A, Fuchs AF (1993) Role of the caudal fastigial nucleus in saccade generation. II. Effects of muscimol inactivation. *J Neurophysiol* 70:1741–1758
- Rottach KG, Das VE, Wohlgenuth W, Zivotofsky AZ, Leigh RJ (1998) Properties of horizontal saccades accompanied by blinks. *J Neurophysiol* 79:2895–2902
- Scudder CA (1988) A new local feedback model of the saccadic burst generator. *J Neurophysiol* 59:1455–1475
- Scudder CA, Fuchs AF, Langer TP (1988) Characteristics and functional identification of saccadic inhibitory burst neurons in the alert monkey. *J Neurophysiol* 59:1430–1454
- Scudder CA, Kaneko CS, Fuchs AF (2002) The brainstem burst generator for saccadic eye movements. A modern synthesis. *Exp Brain Res* 142:439–462
- Sekirnjak C, du Lac S (2002) Intrinsic firing dynamics of vestibular nucleus neurons. *J Neurosci* 22:2083–2095
- Shults WT, Stark L, Hoyt WF, Ochs AL (1977) Normal saccadic structure of voluntary nystagmus. *Arch Ophthalmol* 95:1399–1404
- Soetedjo R, Kaneko CR, Fuchs AF (2002) Evidence that the superior colliculus participates in the feedback control of saccadic eye movements. *J Neurophysiol* 87:679–695
- Sohal VS, Huntsman MM, Huguenard JR (2000) Reciprocal inhibitory connections regulate the spatiotemporal properties of intrathalamic oscillations. *J Neurosci* 20:1735–1745
- Sparks DL (2002) The brainstem control of saccadic eye movements. *Nat Rev Neurosci* 3:952–964
- Strassman A, Highstein SM, McCrea RA (1986a) Anatomy and physiology of saccadic burst neurons in the alert squirrel monkey. I. Excitatory burst neurons. *J Comp Neurol* 249:337–357
- Strassman A, Highstein SM, McCrea RA (1986b) Anatomy and physiology of saccadic burst neurons in the alert squirrel monkey. II. Inhibitory burst neurons. *J Comp Neurol* 249:358–380
- Sylvestre PA, Galiana HL, Cullen KE (2002) Conjugate and vergence oscillations during saccades and gaze shifts: implications for integrated control of binocular movement. *J Neurophysiol* 87:257–272
- Van Gisbergen JA, Robinson DA, Gielen S (1981) A quantitative analysis of generation of saccadic eye movements by burst neurons. *J Neurophysiol* 45:417–442
- Wong AM, Musallam S, Tomlinson RD, Shannon P, Sharpe JA (2001) Opsoclonus in three dimensions: oculographic, neuropathologic and modelling correlates. *J Neurol Sci* 189:71–81
- Yee RD, Spiegel PH, Yamada T, Abel LA, Suzuki DA, Zee DS (1994) Voluntary saccadic oscillations, resembling ocular flutter and opsoclonus. *J Neuroophthalmol* 14:95–101
- Zee DS, Hain TC (1992) Clinical implications of otolith-ocular reflexes. *Am J Otol* 13:152–157
- Zee DS, Robinson DA (1979) A hypothetical explanation of saccadic oscillations. *Ann Neurol* 5:405–414
- Zee DS, Fitzgibbon EJ, Optican LM (1992) Saccade-vergence interactions in humans. *J Neurophysiol* 68:1624–1641